OPTIMIZING MESH CONFIGURATIONS IN SOLAR CHIMNEY SYSTEMS: A COMPUTATIONAL FLUID DYNAMICS (CFD) BASED APPROACH FOR ENHANCED ENERGY EFFICIENCY AND

Environmental Engineering and Management Journal

July 2025, Vol. 24, No. 7, 1509-1519
http://www.eemj.icpm.tuiasi.ro/; http://www.eemj.eu
http://doi.org/10.30638/eemj.2025.118

"Gheorghe Asachi" Technical University of Iasi, Romania

OPTIMIZING MESH CONFIGURATIONS IN SOLAR CHIMNEY SYSTEMS: A COMPUTATIONAL FLUID DYNAMICS (CFD) BASED APPROACH FOR ENHANCED ENERGY EFFICIENCY AND PERFORMANCE

Jihen Mahdhi[1], Ons Ghriss[2], Humberto Garcia Castellanos[3], Abdallah Bouabidi[1,4], Ali Keçebaş[5], Yashar Aryanfar[6,7]*

[1]Laboratory of Mechanical Modeling, Energy & Materials (LM2EM), LR24ES23, National School of Engineers of Gabes (ENIG), University of Gabes, Avenue of Omar Ib-Elkhattab, Zrig 6023, Gabes, Tunisia
[2]National Engineering School of Gabes (ENIG), Research Laboratory "Processes, Energetics Environment and Electrical Systems", Gabes University, Omar Ibn Kattab ZRIG, Gabes, 6029, Tunisia
[3]Engineering Sciences, Tecnológico Nacional de México IT Ciudad Juárez, Juarez, Chihuahua, Mexico
[4]Higher Institute of Industrial Systems of Gabes, University of Gabes, Tunisia
[5]Department of Energy Systems Engineering, Technology Faculty, Muğla Sıtkı Koçman University, 48000 Menteşe, Muğla, Turkey
[6]Department of Electric Engineering and Computation. Autonomous University of Ciudad Juárez. Av. Del Charro 450 Norte. Col. Partido Romero. Juárez, Chihuahua, México
[7]Thermo-Fluids Research Group, Department of Mechanical Engineering, Khazar University, Baku 1009, Azerbaijan

Abstract

The present study investigates the effect of mesh configurations on the performance of a solar chimney (tower) system using Computational Fluid Dynamics (CFD) simulations. This research focuses on optimizing mesh density to enhance the accuracy of temperature, velocity, and pressure predictions in the solar tower, which significantly impact energy efficiency. Unlike previous studies, which primarily focused on geometrical design and system layout, this article introduces a novel meshing strategy that balances computational efficiency and simulation accuracy. Four different mesh types were analyzed, with the finest meshes (M3 and M4) showing the closest alignment to experimental data, achieving an error margin below 4%. The results revealed that finer meshes provided more accurate representations of temperature profiles, pressure gradients, and velocity distributions, particularly near the chimney's axis, optimizing the overall system's performance. The minimum total pressure values for meshes were 5.61 Pa, 6.25 Pa, 6.61 Pa, and 6.86 Pa, respectively, indicating how mesh density influences internal pressure dynamics. This study highlights the importance of mesh selection in CFD simulations and recommends future designs to incorporate adaptive mesh refinement techniques for better simulation efficiency. The findings offer valuable insights into the design and optimization of solar tower systems, promoting enhanced power generation and efficiency, which are essential for scaling renewable energy projects. Future research could explore broader applications of this methodology to optimize other renewable energy systems.

Key words: Computational Fluid Dynamics, mesh effect, numerical analysis, solar energy, solar tower

Received: August, 2023; Revised final: October, 2024; Accepted: November, 2024; Published in final edited form: July, 2025

* Author to whom all correspondence should be addressed: e-mail: yashar.aryanfar@gmail.com; al216622@alumnos.uacj.mx; Phone: +525626776998

1. Introduction

The concept of a Solar Tower, often referred to as a Solar Chimney, represents a pivotal innovation in renewable energy technology, harnessing the sun's power to generate clean electricity. This paper introduces the fundamental principles and the ground-breaking potential of Solar Tower systems, a technology that offers a sustainable solution to the growing global energy demand. At the heart of this technology lies the simple yet powerful principle of thermodynamics (Ayadi et al., 2018): solar radiation heats the air within a large greenhouse-like structure at the base, causing it to rise through a tall chimney, thereby driving turbines to produce electricity. The Solar Tower's operational mechanism not only exemplifies an elegant blend of architectural design and engineering but also marks a significant step towards achieving a low-carbon future. Furthermore, this elegant synergy between architectural design and engineering principles is also mirrored in the sophisticated design of solar chimneys, where the optimization of solar energy capture and enhancement of energy efficiency are main objectives.

Solar chimney designs epitomize the integration of advanced engineering principles with renewable energy utilization. These structures typically feature a large, circular base leading up to a tall, slender chimney (Fasel et al. 2013). The fundamental mechanism involves solar radiation heating the air at the base of the chimney, causing this warmed air to ascend through the chimney. This upward air movement activates turbines located along the chimney, thereby generating electricity. Solar chimneys are often constructed using transparent materials and may include additional heat collection panels at their base. These designs represent an innovative approach to sustainable energy solutions, focusing on minimizing environmental impact. The intricate geometric configurations of solar chimneys are continually refined to optimize solar energy harnessing and enhance energy efficiency. The sophisticated design and energy-efficient operation of solar chimneys pave the way for the application of Computational Fluid Dynamics (CFD) in enhancing their performance. The use of CFD complements the advanced engineering principles of solar chimney design, bridging the gap between theoretical efficiency and practical application. This synergy of design and analysis not only exemplifies a more refined approach to renewable energy technologies but also underscores the evolving nature of solar energy research (Elakrout et al., 2024).

CFD plays a pivotal role in the design of solar chimneys, serving as a crucial tool for optimizing their efficiency and performance. CFD enables detailed modeling of air flow and heat transfer within solar chimneys, allowing engineers to predict the velocity of air flow, temperature distribution, and energy generation by turbines with high precision. These simulations assist in the optimization of geometric parameters such as chimney height, diameter, and shape, thus enabling designers to develop more efficient and effective solar chimney designs (Muhammed and Atrooshi, 2019). Furthermore, CFD analysis identifies potential airflow obstructions and temperature gradients within the chimney design, aiding in reducing energy losses and enhancing overall system efficiency. In this context, CFD emerges as an indispensable technology in the design and development of sustainable energy systems, facilitating nuanced understanding and improvement of solar chimney functionalities. In recent years, several studies have been reported encouraging the use of solar towers to generate electricity, and the number of studies interesting in computational methods has increased to study the solar setup. Using the CFD code, Mebarki et al. (2022) created a numerical model. All models were validated by comparing the developed models to the experimental data from the SCPP in Manzanares, Spain. They observed that while temperature increases logarithmically, the air velocity, mass flow rate, pressure difference, linear, and polynomial decrease as the scale factor decreases. To investigate the performance parameters of a sloped collector in the SCPP, Weli et al. (2021) presented a novel numerical model. In their research, they used a 3D CFD simulation to estimate the geometrical parameters of the solar tower. The findings indicated that a better configuration had a collector cover tilt of 0 ° parallel to the ground. The effect of building storey count on solar chimney power plant performance was investigated by Zhang et al. (2022) using theoretical and computational methods. Several numerical models were run by Azad et al. (2021) to optimize the chimney's design, including the chimney's height, diameter, and collector diameter. The numerical outcomes demonstrated how the various geometric parameters under investigation impact the solar tower's performance. In their work, Zuo et al. (2021) designed a wind turbine for a solar tower using the axial-flow hydraulic turbine impeller's lifting design method, and they investigated how solar radiation affected the turbine. The thermal performance of the solar tower system was examined and optimized by Praveen et al. (2021). In addition to the three crucial parts, a collector, chimney, and turbine, a bell-mount inlet is also suggested. The findings demonstrated that incorporating an effective bell mouth at the inlet and making appropriate design alterations to the collector and chimney could significantly enhance air velocity by roughly 270%. A thorough examination of the design and performance analysis of the solar chimney power plant was reported by Pradhan et al., (2021). Using CFD and ANN models, Cuce et al. (2024) examined the effects of collector slope and chimney divergence angle on the operation of solar chimney power plants. According to their research, power output was greatly increased with a collector slope of 0.6° and a chimney angle of 1.5°, reaching 216.853 kW a 4.5-fold increase over the reference situation. Mandal et al. (2024a) optimized a Manzanares solar

chimney plant by modifying the collector inlet height, chimney diameter, and divergence. They achieved a significant power increase to 635.02 kW by reducing the collector inlet height and expanding the chimney diameter, using an ANN model to accurately predict performance.

A numerical analysis was carried out by Mandal et al. (2024b) to assess the effect of different chimney layouts and shapes on SCPP performance. They discovered that power generation is much increased with an ideal chimney divergence angle of +0.75° and a sloped ground absorber of 0.6°. In particular, the sloped absorber boosted power by 60% (82 kW) while the diverging chimney increased power by 47% (76 kW). When these upgrades were combined, the output reached 92 kW, an 80% increase over the output of the traditional Manzanares plant. In their study, Biswas et al. (2023) investigated the use of a stair-shaped ground absorber in the optimization of a solar tower According to their research, compared to a flat surface, this design can boost power generation by up to 80%, from 51 kW to 92 kW. The study shows that plant efficiency is further enhanced by raising the absorber height or number of steps. This novel method offers important new insights into optimizing solar tower performance and implies that the stair-shaped absorber is a viable substitute for improving power generation. Mandal et al. (2023) investigated improving the efficiency of solar chimney power plants (SCPP) by altering the absorber surface to include triangular wavy peaks with varying amplitudes. They observed a 58.61% increase in power generation, reaching up to 82.5 kW, and a 61.83% improvement in efficiency with higher amplitude waves. Cuce et al. (2024) discovered that a 4.5-fold increase in SCPP power production, to 216.853 kW, could be achieved by adjusting the collection slope and chimney angle. Mandal et al. (2024a) improved the output to 635.02 kW by modifying the chimney diameter and collector inlet height. Additionally, they demonstrated that sloping absorbers and optimal chimney divergence can increase output by up to 80% to 92 kW. Stepper-shaped absorbers have been shown by Biswas et al. to improve power by 80%, whereas Mandal et al. (2023) recorded a 58.61% power gain with triangular wavy absorber surfaces. Our work demonstrates how accurate mesh configurations considerably increase the accuracy of temperature, pressure, and velocity predictions areas not as thoroughly explored in prior studies by combining mesh optimization in CFD simulations for solar tower in a novel way. This method provides fresh perspectives on how to get performance evaluations for solar tower systems that are more precise and trustworthy. These researches underscore the complexity and intricacy of mesh structures in the geometries of solar chimney designs. The diverse approaches and optimizations highlighted in these studies reflect the significant challenge of accurately modelling air flow and thermal dynamics within these systems. This complexity not only demands precision in computational modelling but also emphasizes the need for advanced meshing techniques to effectively capture the nuanced variations in geometrical parameters and their substantial impact on the overall performance of solar tower systems.

This article distinguishes itself from the existing literature by presenting a novel approach to the design and optimization of solar chimney systems. While previous studies, as referenced above, have significantly contributed to the understanding of solar tower performance and design optimization, this paper introduces an innovative methodology that combines advanced computational techniques with new material applications. Specifically, the focus of this study is on exploring alternative materials for the collector and chimney, as well as employing a unique meshing strategy in CFD simulations to enhance accuracy and efficiency. The methodology involves a comprehensive analysis of thermal dynamics and fluid flow, integrating both theoretical and practical perspectives to optimize the design parameters of solar chimneys. By doing so, this work aims to not only contribute to the existing body of knowledge but also to propose practical solutions that can be adopted in the real-world implementation of solar chimney power plants, thereby advancing the field towards more sustainable and efficient energy systems.

2. Materials and method

2.1. Geometrical modelling and numerical analysis

In this study, the scope extends beyond geometric design to encompass the development and evaluation of four different types of mesh. This step is essential for verifying the accuracy of numerical results against experimental data, a critical aspect in ensuring the reliability and effectiveness of the geometric structure built at the University of Suva in Fiji. The University of Suva in Fiji has constructed a geometric structure based on the dimensions similar to those described by Ahmed and Patel (2017). Fig. 1 shows its key structure. This structure is situated in Fiji City, which is located at a longitude of 178.44° East and a latitude of -18.14° South. Main features of this structure include a stack height of 4 m and a convergence angle of 2 °, coupled with a collector diameter of 3.2 m. These dimensions and angles were carefully selected to optimize the structure's functionality and efficiency, reflecting the findings of Ahmed and Patel (2017)'s research. The boundary conditions applied in the simulation are summarized in Table 1, which presents detailed information about the conditions for the chimney, glass cover, inlet, outlet, and ground surfaces.

Table 1 presents a detailed overview of the various materials utilized in the construction of this solar tower, highlighting their distinct characteristics. The following are thorough explanations of the boundary conditions. For the simulation, relative static pressure was employed to examine the system's whole pressure distribution.

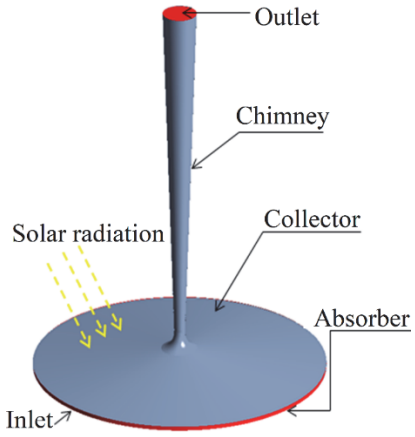

Fig. 1. Solar tower prototype

Table 1. Boundary conditions

Boundary	***Conditions***
Chimney	Adiabatic wall, Q= 0 W/m^2
Glass cover	Semi-transparent wall, h= 10 W/m^2.k
Inlet	Pressure inlet, ΔP= 0 Pa, T= 304 K
Outlet	Pressure outlet, ΔP= 0 Pa, T= 304 K
Ground	Mixed, T= 323 K

There was zero Pa of relative static pressure between the collector input and chimney output. Heat flux was the term used to describe solar radiation that warms the ground beneath the canopy. The energy that the ground absorbs, and the energy lost through radiation and conduction have been considered. The University of Suva in Fiji set the solar radiation to 1000 W/m^2 by average solar radiation circumstances. The experiments were conducted under specific environmental conditions: the ambient temperature was maintained at 304 K, and the weather was sunny, characterized by a global solar radiation of 1000 W/m^2. These conditions are essential to understand as they significantly impact the tower's performance. The fundamental equations governing the system, including the principles of continuity, momentum conservation, and energy conservation, are crucial for a comprehensive analysis. The practical application needs influenced the selection of researched parameters in this research, which concentrated on mesh density and turbulence models. In order to ensure practical implementation in large-scale simulations, mesh density was adjusted to strike a balance between computational efficiency and simulation accuracy.

The dependability of advanced turbulence models in capturing flow dynamics led to the selection of models such as RNG k-epsilon. For best thermal performance, solar radiation is correctly modeled by solar ray tracing methods like the discrete ordinates (DO) approach. These specifications, which include geometric elements like chimney diameter and collector height, were chosen specifically to affect and enhance the solar tower's power output and efficiency. These equations are formulated as follows, as referenced in Hassan et al., (2018), providing a theoretical framework for understanding the complex interactions within the solar tower system (Eqs. 1-5).

- The continuity Equation (1):

$$\frac{\partial(\rho u)}{\partial x}+\frac{\partial(\rho v)}{\partial y}+\frac{\partial(\rho w)}{\partial z}=0 \quad (1)$$

- The momentum Equations (2-4):

$$\frac{\partial(\rho uu)}{\partial x}+\frac{\partial(\rho uv)}{\partial y}+\frac{\partial(\rho uw)}{\partial z}=-\frac{\partial P}{\partial x}+\frac{\partial}{\partial x}\left(\mu\frac{\partial u}{\partial x}\right)+\frac{\partial}{\partial y}\left(\mu\frac{\partial u}{\partial y}\right)+\frac{\partial}{\partial z}\left(\mu\frac{\partial u}{\partial z}\right) \quad (2)$$

$$\frac{\partial(\rho uv)}{\partial x}+\frac{\partial(\rho vv)}{\partial y}+\frac{\partial(\rho vw)}{\partial z}=-\frac{\partial P}{\partial y}+\frac{\partial}{\partial x}\left(\mu\frac{\partial v}{\partial x}\right)+\frac{\partial}{\partial y}\left(\mu\frac{\partial v}{\partial y}\right)+\frac{\partial}{\partial z}\left(\mu\frac{\partial v}{\partial z}\right) \quad (3)$$

$$\frac{\partial(\rho uw)}{\partial x}+\frac{\partial(\rho uw)}{\partial y}+\frac{\partial(\rho ww)}{\partial z}=-\frac{\partial P}{\partial z}+\frac{\partial}{\partial x}\left(\mu\frac{\partial w}{\partial x}\right)+\frac{\partial}{\partial y}\left(\mu\frac{\partial w}{\partial y}\right)+\frac{\partial}{\partial z}\left(\mu\frac{\partial w}{\partial z}\right)+\rho_0 g\beta(T-T_{ref}) \quad (4)$$

- The energy Equation (5):

$$\frac{\partial(\rho uT)}{\partial x}+\frac{\partial(\rho vT)}{\partial y}+\frac{\partial(\rho wT)}{\partial z}=\frac{\partial}{\partial x}\left(\frac{\lambda}{C_p}\frac{\partial T}{\partial x}\right)+\frac{\partial}{\partial y}\left(\frac{\lambda}{C_p}\frac{\partial T}{\partial y}\right)+\frac{\partial}{\partial z}\left(\frac{\lambda}{C_p}\frac{\partial T}{\partial z}\right) \quad (5)$$

The power calculation for each area of the solar tower has been approached in various ways in the literature. In this study, the power is calculated using the efficiency (η), surface area (A), and solar irradiance (I), by the following equation (Mandal et al., 2024a):

Collector area (Eqs. 6-8):

$$P_{collector}=\eta_{collector}A_{collector}I_{solar} \quad (6)$$

where: $\eta_{collector}$ is the efficiency of the collector, $A_{collector}$ is the area of the collector (m²), and I_{solar} is the solar radiation (W/m²).

$$\eta_{collector}=\frac{\dot{Q}_{collector}}{A_{collector}I_{solar}} \quad (7)$$

$$\dot{Q}_{collector}=\dot{m}C_p(T_{out}-T_{in}) \quad (8)$$

where: $\dot{m}$ is the mass flow rate of the air, C_p is the specific heat capacity of air (kJ/kgK), and T_{out} and T_{in} are outlet and inlet temperatures of the air (K), respectively.

Absorber area (Eqs. 9-11):

$$P_{absorber}=\eta_{absorber}A_{absorber}I_{solar} \quad (9)$$

$$\eta_{absorber}=\frac{\dot{Q}_{absorber}}{A_{absorber}I_{solar}} \quad (10)$$

$$\dot{Q}_{absorber}=\dot{m}C_p(T_{absorber\_out}-T_{absorber\_in}) \quad (11)$$

where: $\dot{Q}_{absorber}$ is the heat gained by the air due to the absorber surface (W),

$T_{absorber\_out}$ and $T_{absorber\_in}$ are the outlet and inlet temperature of the air interacting with the absorber surface (K), and $A_{absorber}$ is the area of the absorber surface (m²).

Chimney (Eq. 12):

$$P_{chimney} = \eta_{chimney} \rho g \dot{V} h \quad (12)$$

where: $\eta_{chimney}$ is the efficiency of the chimney, ρ is the air density (kg/m³), g is the gravitational acceleration (m/s²), $\dot{V}$ is the volumetric flow rate (m³/s), and h is the height of the tower (m).

$$\eta_{chimney} = \frac{P_{chimney}}{\dot{Q}_{chimney}} \quad (13)$$

$$P_{chimney} = \frac{1}{2} \dot{m} v_{chimney}^2 \quad (14)$$

$$\dot{Q}_{chimney} = \dot{m} C_p (T_{collector\_out} - T_{ambient}) \quad (15)$$

where: $\dot{Q}_{chimney}$ is the thermal power input (W), $v_{chimney}$ is the velocity of the air in the chimney (m/s), and $T_{ambient}$ is the ambient temperature (K).

Table 1 is summarized the results for the power generated by each area.

Table 1. Power generation by different area

Area	*Power rate (W)*
Collector	1552.799
Absorber	1212.992
Chimney	30.494

Dimensionless parameters are crucial in the analysis of fluid flow and heat transfer as they contribute to the generalization of results and facilitate the comparison between different systems. In this study, the most important dimensionless parameters include (Nasraoui et al. 2020).

Rayleigh Number (Ra): This number assesses the strength of buoyancy-driven flow by combining the effects of thermal expansion and temperature gradient, The Rayleigh number is defined as Eq. (16):

$$Ra = \frac{g\beta(T_h - T_c)L^3}{v\alpha} \quad (16)$$

The Nusselt number (Nu): It measures the effectiveness of convective heat transfer relative to conductive heat transfer, providing insight into heat transfer efficiency and is written as Eq. (17):

$$N_u = \frac{hL}{k} \quad (17)$$

The Reynolds number (Re): This parameter indicates the ratio of inertial forces to viscous forces, which helps determine whether the flow (Eq. 18).

$$Re = \frac{\rho u L}{\mu} \quad (18)$$

The Prandtl number (Pr): It represents the ratio of the momentum diffusivity to the thermal diffusivity.

$$Pr = \frac{v}{\alpha} \quad (19)$$

The assumptions that closely align with the numerical conditions are as follows:

- The air flow within the solar chimney is assumed to be incompressible.
- The system is assumed to operate under steady-state conditions.
- The Boussinesq approximation is applied to account for buoyancy effects.
- All fluid properties are held at constant values.
- The density behaves similarly to that of an ideal gas.

2.2. Mesh generation

In fluid dynamics simulations, creating a mesh accurately is crucial, particularly with complex shapes. The precision of the mesh significantly influences the simulation results, regardless of the software used. Considering computer memory availability is also important, especially for detailed areas like micro grids. This study examines various mesh types, drawing insights from Ahmed and Patel (2017)'s research. Meshes generally fall into two categories: structured and unstructured. An unstructured polyhedral mesh was selected for its balance in handling geometric complexities. This mesh type is both easier and more efficient to create than others, requiring minimal surface preparation. It consists of cells of varying sizes, strategically smaller in areas with significant temperature and movement changes, ensuring detailed results in those regions.

2.3. Optimizing the Mesh for SCPP

Optimizing the mesh is essential to improving the precision and effectiveness of simulations for Solar Tower. It is necessary to thoroughly improve critical areas like the chimney, the collector area, and the collector intake. In these regions, a finer mesh better captures the sudden variations in pressure, temperature, and velocity.

Mesh density can be dynamically adjusted via Adaptive Mesh Refinement (AMR) in response to flow parameters, and hybrid mesh techniques, which combine structured and unstructured meshes, provide a computationally efficient yet accurate solution. The design and operation of effective SCPP are aided by this optimization, which makes forecasts more insightful and dependable.

3. Results and discussion

In this study, the focus is on analysing numerical mesh results based on the experimental

work of Ahmed and Patel (2017). Four different types of meshes were created to identify the most effective one for comprehensive simulations. The findings and their detailed discussions are presented in the subsequent sections, offering an in-depth analysis of each mesh type and its impact on the overall simulation accuracy.

Ansys Fluent software is used in our numerical process to solve the governing equations of fluid flow and heat transport. Determining the geometry and creating the computational mesh are the first steps in the process. In order to accurately imitate the physical world, boundary conditions are used. The turbulence, heat transfer, and fluid flow modeling are then handled by the solver, which is set up to iterate until a convergent solution is obtained.

In our simulations, we use the finite volume method to discretize the governing equations (Navier-Stokes equations and energy equation). This method ensures the conservation of mass, momentum, and energy within each control volume, the iterative process is continued until the residuals are reduced to 10^{-6}.

3.1. Mesh characteristics and their impact on simulation accuracy

The mesh parameters for each type, highlighting the number of cells and nodes presented in Table 2. Specifically, Mesh M1 contains 85,572 cells and 416,283 nodes, representing the simplest mesh with the lowest level of detail. To facilitate the comparison of different mesh configurations, Table 2 provides the number of cells and nodes for each mesh type, demonstrating how increasing mesh density impacts computational resources and simulation accuracy. This mesh is suitable for less complex simulations due to its lower computational demand. Mesh M2, with 162,514 cells and 794,685 nodes, offers a balance between detail and computational efficiency. This mesh could be optimal for moderately complex simulations. Moving to a higher level of detail, Mesh M3 includes 294,310 cells and 1,254,023 nodes. This mesh is particularly useful for simulations requiring precise details in complex geometries. Lastly, Mesh M4, the most detailed mesh, consists of 483,301 cells and 2,575,438 nodes. This high level of detail is crucial for the most complex simulations, where accuracy is paramount, but it also demands significant computational resources.

Table 2. Comparative overview of mesh types – cell and node counts

Meshing	***M1***	***M2***	***M3***	***M4***
Cells number	85572	162514	294310	483301
Nodes number	416283	794685	1254023	2575438

Figure 2 illustrates the mesh configuration in the solar tower's plane, comparing four mesh densities (M1 to M4). Each mesh is characterized by its cell and node count, directly influencing the simulation accuracy of temperature, pressure, and velocity distribution within the tower. A denser mesh offers better resolution at the cost of higher computational demand. Based on these results, the choice among these meshes depends on the specific requirements of the simulation. A more detailed mesh like M4 provides higher accuracy but requires more computational power and memory. In contrast, Mesh M1, with fewer cells and nodes, is a quicker and less resource-intensive option.

Therefore, the selection of the appropriate mesh should balance the need for accuracy with available computational resources. For instance, while Mesh M4 offers the highest resolution and detail, it may not be necessary for all types of simulations. The decision should be guided by the specific objectives of the simulation and the constraints of the computational environment.

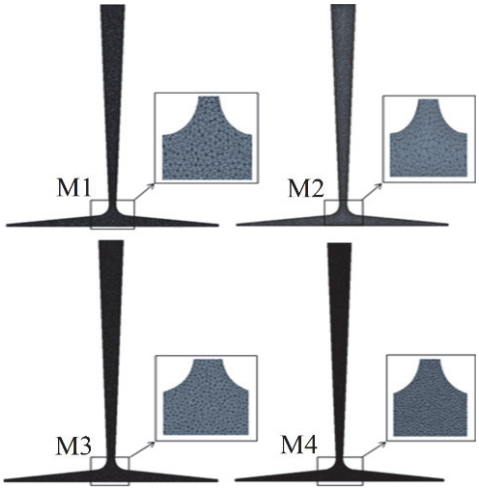

Fig. 2. Visualization of different mesh numbers in the plane

For effective CFD simulations, it is essential to optimize the local mesh size in critical sections of a solar tower. This provides correct capture of complicated flow and thermal behaviours, which improves performance forecasts.

- Chimney: Because of buoyancy, the airflow in the chimney accelerates and there are notable temperature and pressure variations. The total power output and the precision of these forecasts are affected by the mesh size. To accurately represent the performance of the chimney and the outflow circumstances, a small mesh is required to resolve boundary layers along the chimney walls and capture the quick changes in flow parameters.
- Collector inlet: The system ambient air enters through the collector intake, where it quickly changes in temperature and velocity. This region benefits from a finer mesh since it catches these changes more precisely, allowing for accurate initial airflow condition prediction. Increased modelling of the collector's following air flow and heating results from this.

• Collector: The ground absorber heats the air inside the collector, here, changes in mesh size have an impact on the thermal and velocity field predictions. Realistic simulation results are ensured by a dense mesh, which accurately represents the temperature rise and velocity increase, especially near the collector centre where maximal heating takes place.

The CFD simulations demonstrated that finer mesh configurations, particularly M3 and M4, provided a more accurate representation of temperature profiles, closely aligning with the experimental data. These finer meshes were essential in capturing the subtle variations in temperature, especially at critical points in the solar tower system. Moreover, the pressure distribution was significantly influenced by mesh density, with M3 and M4 showing more reliable results in predicting the pressure gradients, which play a pivotal role in the energy conversion processes within the chimney. The velocity distribution along the chimney axis also exhibited distinct patterns depending on the mesh density. The higher-density meshes, such as M3 and M4, were better at predicting peak velocity values, which is crucial for optimizing turbine placement and overall system efficiency. These findings underscore the importance of selecting the appropriate mesh configuration to ensure simulation accuracy and reliability in predicting the physical behavior of the solar tower system.

3.2. Temperature distribution analysis

In this study, an essential aspect is the selection of the most suitable mesh based on temperature analysis. To achieve this, a comparative analysis of temperature distributions across four different mesh types was conducted. Fig. 3 provides a visual representation of these comparisons, showcasing the temperature contours within the solar tower for each mesh. This comparison is pivotal in understanding how variations in mesh size influence the overall temperature distribution within the simulation. Temperature distribution was analyzed across different mesh types, with M3 and M4 showing the closest alignment to experimental data (Fig. 4). These finer meshes provided a more accurate representation of the temperature profile within the solar tower.

Figure 4 shows how mesh density affects heat distribution inside the collector. A critical observation from Fig. 4 is the consistent pattern of maximum temperatures occurring in the absorber across all mesh types. However, it is the alignment with experimental data that truly determines the appropriateness of each mesh. In this regard, air temperature profiles from the collector for the different meshes were integrated with the experimental data obtained from Ahmed and Patel (2017). This integration allows for a direct comparison between the computational fluid dynamics (CFD) simulation results and the established experimental benchmarks. The findings reveal a close correlation between the temperature profiles of the third and fourth meshes and the experimental data, with the first and second meshes displaying notable deviations from the experimental results. Given this, the decision was narrowed down to choosing between the third and fourth meshes.

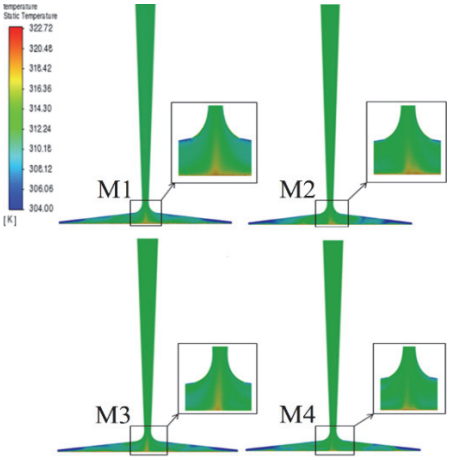

Fig. 3. Temperature distribution across the solar tower in the plane

Despite their similar accuracy in replicating the experimental temperature profiles, the third mesh was favoured due to its shorter simulation time. Opting for the third mesh means achieving a balance between computational efficiency and accuracy, with an error margin maintained below 4%. This strategic choice underscores the importance of optimizing mesh selection not only for accuracy but also for computational practicality in complex CFD simulations.

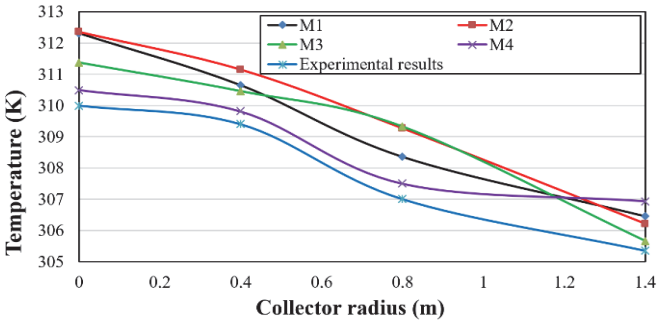

Fig. 4. Comparative temperature profiles in the collector

3.3. Velocity magnitude variations

Figure 5 shows the magnitude of velocity distribution within the solar tower system, specifically along the collector and the chimney, for the different meshes. A comparison of the velocity distribution along the chimney's axis highlights the distinct differences among the four mesh types. Velocity variations, especially along the chimney axis, were most accurately captured with finer meshes, such as M3 and M4, as seen in Fig. 5. The maximum velocity values were observed near the collector output, where

significant pressure differentials occur. This comparison reveals that the maximum and minimum values of velocity magnitude for the various scenarios are consistently located at identical points in the system. The velocity is notably significant along the axis of the chimney, especially near the collector output close to the axis, where it reaches its peak at the junction. This occurrence is attributed to the pressure differential, which is most pronounced in this area.
Further analysis shows that the magnitude of velocity decreases across the collection radius, with the lowest values observed at the collector intake. Interestingly, the highest velocity values are found to vary depending on the specific mesh configuration used. Comparing these results highlights the direct influence of the different meshes on the velocity magnitudes within the solar tower.

This analysis is crucial for understanding how mesh selection impacts the overall fluid dynamics of the system, particularly in terms of velocity distribution and pressure variations.

3.4. Pressure distribution analysis

The total pressure distribution within the solar tower is analysed using various mesh configurations. Figure 6 presents a detailed visualization of this pressure distribution for the different mesh types used in the study. It is observed that there is a uniform pressure distribution under the roof and throughout the glass covering of the tower. This uniformity in pressure gradually decreases as one moves towards the chimney inlet, indicating a shift in pressure dynamics within the structure.
At the base of the tower, particularly close to the wall, a notable depression zone is identified. This area is critical in understanding the pressure variations within the tower. The data from the different mesh configurations, specifically M1 with 416,283 nodes, M2 with 794,685 nodes, M3 with 1,254,023 nodes, and M4 with 2,575,438 nodes, reveal interesting patterns.

The minimum total pressure values for these meshes are found to be 5.61 Pa for M1, 6.25 Pa for M2, 6.61 Pa for M3, and 6.86 Pa for M4, respectively. To further enhance clarity, key numerical trends and values, such as minimum pressure values for each mesh (M1: 5.61 Pa, M2: 6.25 Pa, M3: 6.61 Pa, M4: 6.86 Pa), were summarized in Table 2, enabling a more accessible comparison of mesh impacts. These values provide insight into how the density of the mesh impacts the pressure readings at critical points within the tower. On the other hand, the compression zone, located at the tower's output, exhibits maximum pressure values. Interestingly, across all different mesh configurations, this maximum value is consistently 0.03 Pa. This uniformity in the compression zone's maximum pressure values regardless of the mesh density highlights a unique aspect of the tower's pressure dynamics.

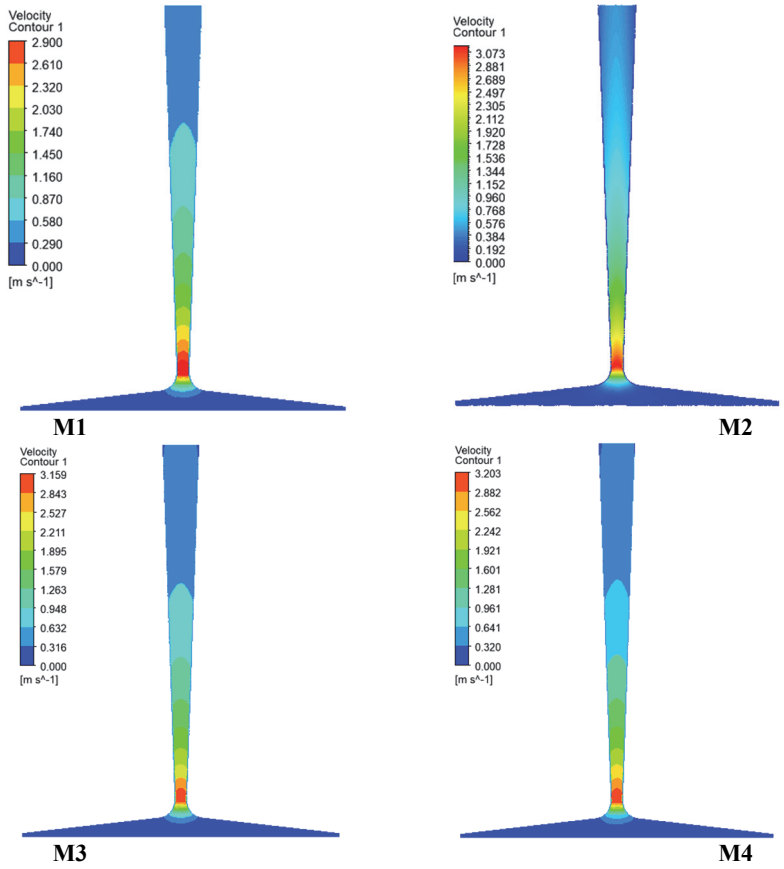

Fig. 5. Visualization of velocity distribution in the tower's plane

To address the potential asymmetric features in the flow structure, a detailed analysis was conducted on the velocity, pressure, and temperature distributions throughout the solar tower. The CFD simulations revealed that the overall flow structure remains largely symmetric along the vertical axis of the chimney, with no significant asymmetries observed in the bulk flow patterns. However, minor localized variations in flow velocity and pressure were noted near the collector inlet and along the chimney walls. These variations are attributed to boundary layer effects and minor temperature gradients within the system. Importantly, these localized deviations do not extend beyond specific regions and do not significantly impact the overall symmetry of the flow. The mesh refinement process, particularly with the use of higher-density meshes (M3 and M4), was critical in minimizing any potential asymmetries and improving the alignment of simulation results with experimental data. As a result, it can be concluded that the system operates with symmetric flow characteristics under the tested conditions, ensuring uniformity in energy conversion and overall system performance. Therefore, no significant asymmetric features were found that would affect the performance or functionality of the solar tower system. A comparative analysis of these results clearly demonstrates that the different mesh configurations have a direct and measurable impact on the pressure distribution inside the solar tower. Such insights are crucial for optimizing the design and functionality of solar tower systems, ensuring that pressure dynamics are accurately accounted for in various simulation scenarios.

The impact of mesh configuration on the total pressure distribution further highlights the importance of mesh refinement in CFD simulations. In particular, the finer meshes M3 and M4 demonstrated their ability to capture the pressure variations at critical points, such as the chimney inlet and outlet. This precision is crucial for optimizing the solar tower design, as accurate pressure predictions directly affect the performance of the system.

The uniformity in the pressure distribution across all mesh configurations at the tower's output confirms that the primary pressure dynamics are mesh-independent, while the variations at the inlet and along the chimney are highly sensitive to mesh density. This detailed analysis reinforces the need for careful consideration of mesh density in future design and simulation efforts to enhance the reliability and efficiency of solar tower systems. Using optimal mesh configurations and advanced turbulence modeling (RNG k-epsilon model and DO solar ray tracing technique) for CFD simulations in solar tower this study extends previous research.

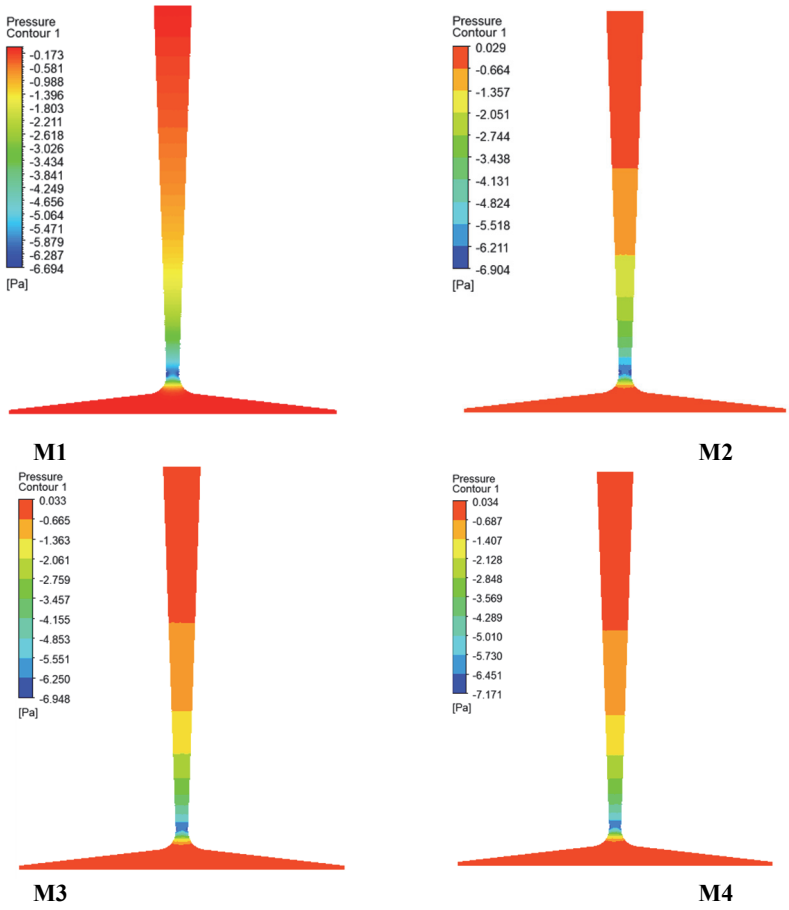

Fig. 6. Detailed pressure distribution in the tower's plane

It investigates the effects of geometric changes that lead to considerable increases in power production, such as collector slope and chimney divergence angle. These aspects together offer a more thorough method of optimizing soar tower designs than any previous research has managed to accomplish.

The results provide important information for increasing the power production and efficiency of solar tower, increasing their viability and cost-effectiveness for large-scale renewable energy projects. In addition to helping with thermal engineering and other fields of fluid dynamics, the latest CFD simulation techniques can also help industry optimize their systems and improve their performance.

The study conclusions can greatly raise the effectiveness and performance of solar tower and give engineers a road map for better operation and design. By applying these developments to practical engineering projects, power generation in solar power plants can be enhanced and costs can be decreased, making renewable energy sources more competitive and lowering greenhouse gas emissions. Innovation across sectors can be fostered by adapting the improved designs and processes to additional sources of renewable energy and industrial uses.

4. Conclusions

In this study, a numerical investigation has been conducted to examine the impact of mesh configurations on a solar tower system. The study successfully developed a numerical model that closely mirrors real-world conditions, enabling a comprehensive comparison with the experimental findings from literature. This paper presents numerical profiles for temperature, velocity, and static pressure distributions within the solar chimney and across various planes, considering different mesh node counts. The following insights, outlined below, can guide readers to significant conclusions drawn from this study:

- The most detailed mesh, M4, contains 483,301 cells and 2,575,438 nodes, offering the necessary high level of detail for the most complex simulations. Conversely, Mesh M1, suitable for less complex simulations, contains 85,572 cells and 416,283 nodes, requiring fewer computational resources.
- The temperature profiles of the third and fourth meshes closely aligned with the experimental data from literature. These meshes contain 294,310 and 483,301 cells, respectively, whereas the first and second meshes showed significant deviations from the experimental results.
- The magnitude of velocity showed distinct variations across different meshes within the tower, particularly along the axis of the chimney. The highest velocity values varied depending on the mesh configuration, indicating the influence of mesh density on fluid dynamics.
- Different mesh configurations directly impacted the total pressure distribution inside the solar tower. The minimum total pressure values for the meshes M1, M2, M3, and M4 were measured at 5.61 Pa, 6.25 Pa, 6.61 Pa, and 6.86 Pa, respectively.
- Across all mesh configurations, the maximum pressure value at the tower's output was consistently measured at 0.03 Pa. This finding highlights a unique aspect of the tower's pressure dynamics, independent of mesh density.
- Increasing the chimney height, optimizing the collector slope to 0.6°, and setting the chimney divergence angle to 1.5° enhance air velocity and power output significantly. Additionally, using high-density meshes like M3 or M4 and fine-tuning flow control parameters, such as air inlet temperature and chimney diameter, maximize thermal efficiency and improve overall system performance.

In light of the findings from this study, it is recommended that future research and practical applications in solar tower systems focus not only on mesh optimization but also on broader design aspects such as chimney height, collector slope, and chimney divergence angle. Implementing adaptive mesh refinement (AMR) techniques and optimizing system geometries can significantly enhance power generation and efficiency.

The significant impact of mesh density on temperature, velocity, and pressure distributions within the solar tower underscores the necessity of optimizing mesh in conjunction with system design improvements, ensuring a balance between computational resources, simulation accuracy, and overall system performance.

Future endeavours should focus on developing more efficient computational methods that can handle higher mesh densities without substantially increasing computational costs. Additionally, there is a potential for exploring adaptive mesh refinement techniques which can dynamically adjust mesh densities in regions of interest, thereby enhancing simulation efficiency and accuracy.

References

Ahmed M.R., Patel S.K., (2017), Computational and experimental studies on solar chimney power plants for power generation in Pacific Island countries, *Energy Conversion and Management*, **149**, 61-78.

Ayadi A., Nasraoui H., Bouabidi A., Driss Z., Bsisa M., Abid M.S., (2018), Effect of the turbulence model on the simulation of the air flow in a solar chimney. *International Journal of Thermal Sciences*, **130**, 423-434.

Azad A., Aghaei E., Jalali A., Ahmadi P., (2021), Multi-objective optimization of a solar chimney for power generation and water desalination using neural network, *Energy Conversion and Management*, **238**, 114152.

Biswas N., Mandal D.K., Manna N.K., Benim A.C., (2023), Novel stair-shaped ground absorber for performance enhancement of solar chimney power plant, *Applied Thermal Engineering*, **227**, 120466.

Cuce P.M., Cuce E., Mandal D.K., Gayen D.K., Asif M., Bouabidi A., Alshahrani S., Prakash C., Soudagar M.E.M., (2024), ANN and CFD driven research on main performance characteristics of solar chimney power plants: Impact of chimney and collector angle, *Case Studies in Thermal Engineering*, **60**, 104568, http://doi.org/10.1016/j.csite.2024.104568.

Elakrout O., Ghriss O., Bendaikha W., Castellanos H.G., Bouabidi A., Kecebas A., Aryanfar Y., (2024), Simulation of a double-pass solar air collector for radiation effects using computational fluid dynamics (CFD), *Environmental Engineering and Management Journal*, **23**, 1429-1436.

Fasel H.F., Meng F., Shams E., Gross A., (2013), CFD analysis of solar chimney power plants. *Solar Energy*, **98**, 12-22.

Hassan A., Ali M., Waqas A., (2018), Numerical investigation on performance of solar chimney power plant by varying collector slope and chimney diverging angle, *Energy*, **142**, 411-425.

Mandal D.K., Biswas N., Barman A., Chakraborty R., Manna N.K., (2023), A novel design of absorber surface of solar chimney power plant (SCPP): Thermal assessment, exergy and regression analysis, *Sustainable Energy Technologies and Assessments*, **56**, 103039, https://doi.org/10.1016/j.seta.2023.103039.

Mandal D.K., Biswas N., Manna N.K., Gayen D.K., Benim. A.C., (2024a), An application of artificial neural network (ANN) for comparative performance assessment of solar chimney (SC) plant for green energy production, *Scientific Reports*, **14**, 979, https://doi.org/10.1038/s41598-023-46505-1.

Mandal D.K., Biswas N., Manna N.K., Benim A.C., (2024b), Impact of chimney divergence and sloped absorber on energy efficacy of a solar chimney power plant (SCPP), *Ain Shams Engineering Journal*, **15**, 102390, https://doi.org/10.1016/j.asej.2023.102390.

Mebarki A., Sekhri A., Assassi A., Hanafi A., Marir B., (2022), CFD analysis of solar chimney power plant: Finding a relationship between model minimization and its performance for use in urban areas, *Energy Reports*, **8**, 500-513.

Muhammed H.A., Atrooshi S.A., (2019), Modeling solar chimney for geometry optimization. *Renewable Energy*, **138**, 212-223.

Nasraoui H., Driss Z., Kchaou H., (2020), Novel collector design for enhancing the performance of solar chimney power plant, *Renewable Energy*, **145,** 1658-1671.

Pradhan S., Chakraborty R., Mandal D.K., Barman A., Bose P, (2021), Design and performance analysis of solar chimney power plant (SCPP): A review, *Sustainable Energy Technologies and Assessments*, **47**, 101411, https://doi.org/10.1016/j.seta.2021.101411.

Praveen V., Das P., Chandramohan V.P., (2021), A novel concept of introducing a fillet at the chimney base of solar updraft tower plant and thereby improving the performance: A numerical study, *Renewable Energy*, **179**, 37-46.

Weli R.B., Atrooshi S.A., Schwarze R., (2021), Investigation of the performance parameters of a sloped collector solar chimney model–An adaptation for the North of Iraq, *Renewable Energy*, **176**, 504-519.

Zhang H., Tao Y., Zhang G., Li J., Setunge S., Shi L., (2022), Impacts of storey number of buildings on solar chimney performance: A theoretical and numerical approach, *Energy*, **261**, 125200, https://doi.org/10.1016/j.energy.2022.125200.

Zuo L., Dai P., Yan Z., Li C., Zheng Y., Ge Y., (2021), Design and optimization of turbine for solar chimney power plant based on lifting design method of axial-flow hydraulic turbine impeller, *Renewable Energy*, **171**, 799-811.